

# A STUDY ON LANTHANUM HYDROXIDE / GRAPHENE NANOHYBRID

---

**Nadeem Farooq Abbasi**

Research Scholar, Dept. of Chemistry

North East Frontier Technical University

**Dr. Vinesh Kumar**

Associate Professor, Dept. of Chemistry

North East Frontier Technical University

---

## ABSTRACT

Supercapacitors have a higher energy density than conventional capacitors and a higher power density than batteries. Due to these incalculable characteristics, the research community has been drawn to the field of supercapacitors. However, due to the unsatisfactory performance of electroactive materials, commercially available supercapacitors are limited to using carbon-based materials as electrically active materials, which offer a significantly lower energy density than batteries. Consequently, the development of energy devices with a high energy density and power density remains crucial. To increase the specific capacitance, the morphology, structure, and degree of integration of the electroactive material are crucial factors. During the past decade, numerous 1D/2D nanostructured materials with unanticipated properties have been developed. In addition, multicomponent nanostructured hybrids have been reported to not only benefit from the characteristics of each nanostructure, but also inherit the advantages derived from both nanostructures. This contributes to the efficient exploitation of electroactive species, thereby enhancing the electrochemical performance of the entire electrode. As a result of the numerous transition modes involving the 4f shell of their ions, rare-earth materials received some attention, and there has been a great deal of interest in the design and fabrication of lanthanide compounds. As a result of their exceptional optical, magnetic, and electrical properties, they are extensively utilized as up-conversion materials. In recent years, there has been an increase in the use of rare-earth oxides as electrode materials for battery and supercapacitor applications. Recent research trends have centered on reducing rare-earth materials to nanostructures and confining them within a graphene matrix, which confers increased surface area and high conductivity with enhanced cyclic stability.

**KEY WORDS:** *Lanthanum Hydroxide, Graphene Nanohybrid, Supercapacitor.*

---

## 1. INTRODUCTION

The development of sustainable energy technologies is dependent on electrochemical energy storage techniques. It has greater potential than other energy storage methods because it is more efficient, flexible, and modular, as

many recent versions of micro fuel cells and rechargeable lithium batteries demonstrate. As environmental contamination rises, electrochemical energy storage has taken on greater significance, as it can reduce our dependence on finite fossil fuel reserves. As is the case with ocean thermal, wave, and tidal power, geothermal sources are geologically limited and appear to be costly to develop. Renewable energy aids in protecting the environment by significantly reducing carbon emissions. By utilizing renewable energy sources, we reduce our reliance on fossil fuel, gas, and oil reserves, allowing us to avoid rising energy costs and enhance energy security.

Emerging technologies such as fuel cells, large format lithium-ion batteries, electrochemical reactors such as ion transport membranes, and supercapacitors are used to produce lightweight, portable electrochemical power sources that are in high demand by consumers. Their applications include communication devices, electric vehicles (EV), spacecraft, and pacemakers. Consequently, numerous advancements over the past decade have produced a new class of electrochemical power sources known as electrochemical supercapacitors. In addition, significantly enhanced electrical energy storage (EES) systems are necessary to enable the widespread use of hybrid electric vehicles (HEV), plug-in hybrids, etc.

Numerous applications of nanotechnology could lead to significant improvements in renewable energy. Nanotechnology for Solar Energy Collection and Conversion, one of the NNI's Signature Initiatives, aims to enhance photovoltaic electricity generation, solar thermal energy generation and conversion, and solar-to-fuel conversions. The National Renewable Energy Laboratory has created a nanoparticle etching technology that provides photovoltaic cells a roughness that gives them a black appearance and allows them to better absorb solar energy. The energy conversion efficiency of these "black silicon" solar cells set a new world record (18.2%). A technique designed to increase the efficiency of solar thermal energy conversion uses a low-cost, scalable method to create high-performance nanostructured coatings that enable thermal conversion efficiencies of more than 90% and expand the temperature range for heat-transfer fluids to more than 1200° Fahrenheit. Additionally, bio-inspired applications aim to use nanomaterials to directly convert sunlight into fuels or feedstocks for high-value chemical products. Nanoscale semiconductor catalysts and additives have potential for enhancing sunlight-based hydrogen generation from water. These nanoscale catalysts' optical qualities enable the process to utilize a larger spectrum of sunlight. Similarly, by utilizing a wider spectrum of sunlight, nanostructured photovoltaic systems (such as solar cells) may increase the efficiency of converting sunlight into power.

By utilizing the chemical characteristics and substantial surface area of some nanostructured materials, it may be possible to improve hydrogen storage, a major obstacle in fuel cell applications. At least one present prototype

outperforms the energy storage of conventional batteries by 40%, suggesting that nanotechnology has the potential to increase energy storage, a crucial enabling technology for renewable energy.

## 2. RESEARCH METHODOLOGY

### 2.1 X-ray diffraction research

Powder diffraction is therefore ideally adapted for the identification and characterization of polycrystalline phases. Consequently, the X-ray diffraction pattern of a purified substance is similar to a fingerprint. When an X-ray beam strikes an atom, the surrounding electrons begin to oscillate at the same frequency as the beam. In almost all directions, destructive interference will occur, meaning that the combining waves are out of phase and no energy is emitted from the solid sample. However, the atoms in a crystal are arranged in a regular pattern, and constructive interference occurs in only a few orientations. The waves will be in phase, and well-defined X-ray beams will leave the sample in a variety of orientations. Consequently, a diffracted beam is a beam composed of numerous dispersed rays that mutually reinforce one another. A series of X-ray reflections from parallel planes within the crystal. The three integers  $h$ ,  $k$ , and  $l$ , known as indices, specify the orientation and interplanar spacings of these planes.

Chemical analysis is the most common application of particle (polycrystalline) diffraction. This may involve phase identification (search/match), investigation of high/low temperature phases, solid solutions, and determination of the unit cell parameters of novel materials.

Polymer crystalline structure: A polymer is partially crystalline and partially amorphous. The crystalline domains function as a reinforcing grid (similar to the iron framework in concrete) and enhance the performance over a broad temperature range. However, excessive crystallinity causes fragility. The crystallinity components produce precise, narrow diffraction peaks, whereas the amorphous component produces a broad peak (halo). The ratio of these intensities can be used to determine the crystallinity of the material.

Residual tension: Residual stress is the tension that remains in a material after the force that initially caused the stress has been removed. The definition of stress is force per unit area. Positive values represent tensile (expansion) stress, while negative values represent a compressive state. Strain is the deformation per unit of length.

The scan rate and step size were set to  $3^\circ \text{ min}^{-1}$  and  $0.2^\circ$ , respectively. From the corresponding diffraction pattern, the phase and crystallinity of the prepared nanomaterials and nanohybrid electrodes were analyzed.

## 2.2 The technique of Raman spectroscopy

Raman spectroscopy is a spectroscopy technique that relies on the inelastic scattering of monochromatic light, typically from a laser source. In the case of inelastic scattering, the interaction of a sample with monochromatic light results in a change in the particles' frequency. The sample absorbs photons of the laser light, which are then reemitted. The frequency of reemitted photons is shifted upwards or downwards relative to their original monochromatic frequency; this phenomenon is known as the Raman effect. This shift provides information regarding vibrational, rotational, and other low-frequency atomic transitions. Raman spectroscopy can be applied to the examination of solid, liquid, and gaseous samples.

## 2.3 FE-SEM research

A scanning electron microscope (FE-SEM) produces images of a specimen by scanning it with a focused beam of electrons. Electrons interact with electrons in the sample, generating signals that can be detected and contain information about the surface topography and chemical composition of the sample. In general, the electron beam is surveyed in a raster scan pattern, and the beam's position is combined with the detected signal to create an image. SEM can attain a higher resolution than 1 nanometer.

## 3. RESULTS AND DISCUSSION

### 3.1 X-ray diffraction studies

Figure depicts the XRD pattern of the nanohybrid  $\text{La}(\text{OH})_3/\text{G}$ . The diffraction peaks at  $2\theta$  values of 15.62, 27.25, 27.94, 31.50, 39.48, 48.62, and 55.29 are successfully indexed to the (100), (110), (101), (200), (201), (211), and (310) planes of the hexagonal phase of  $\text{La}(\text{OH})_3$  with a space group of P63/m. The XRD pattern obtained was in excellent accord with the JCPDS data (Card no. 83-2034).

In the  $\text{La}(\text{OH})_3/\text{G}$  nanohybrid, the crisp reflection indicates that the graphene enhances the crystalline nature of the  $\text{La}(\text{OH})_3$  nanoflakes without affecting the crystal phase. In addition, the absence of the graphene peak is due to the uniform distribution of  $\text{La}(\text{OH})_3$  on the graphene surface.

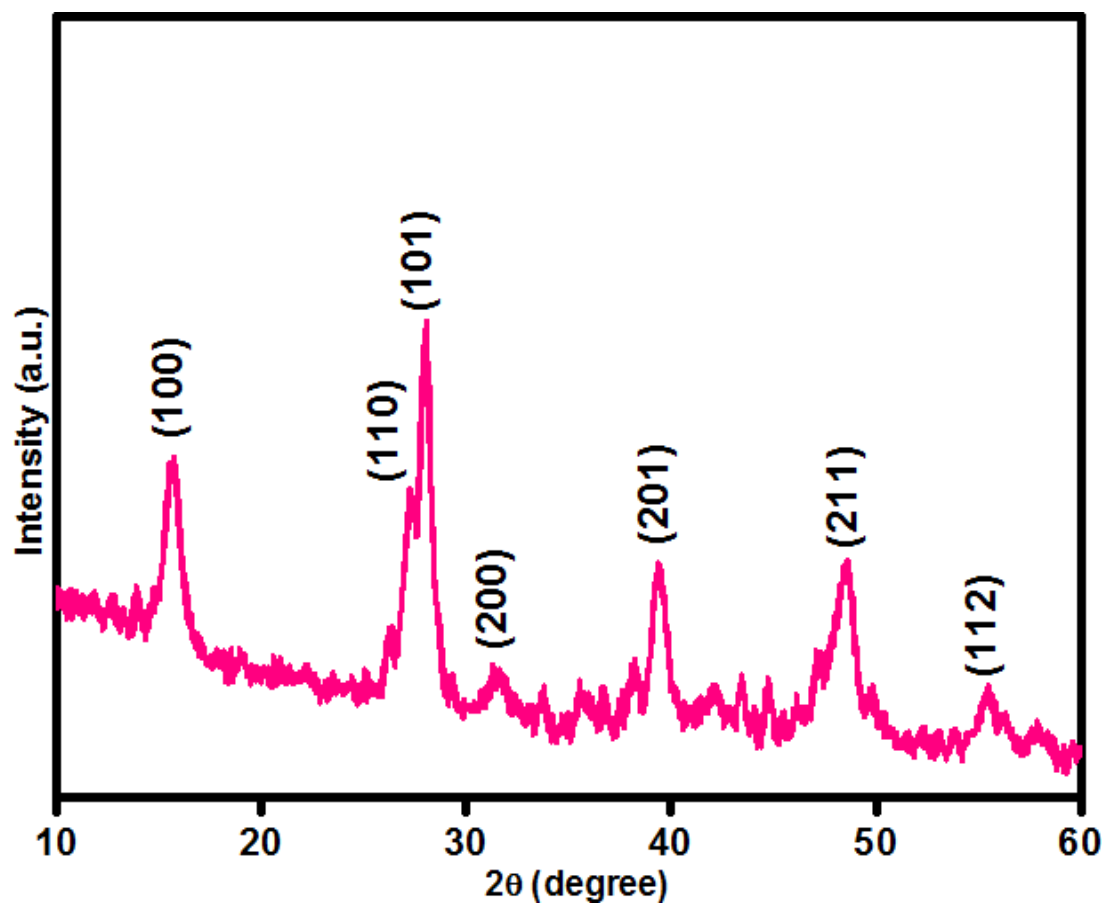


Fig.3.1 . XRD pattern of La(OH)<sub>3</sub>/G nanohybrid.

### 3.2 Raman spectroscopy studies

Figure depicts the Raman spectra of the 2D nanohybrid La(OH)<sub>3</sub>/G. The 2D La(OH)<sub>3</sub>/G nanohybrid exhibits three La(OH)<sub>3</sub> bands at 281 cm<sup>-1</sup>, 337 cm<sup>-1</sup>, and 454 cm<sup>-1</sup> in its Raman spectrum. These Raman modes indicate that La(OH)<sub>3</sub> has formed. The Raman spectrum of 2D La(OH)<sub>3</sub>/G nanohybrid reveals two main graphene peaks, the D and G bands, at 1314 cm<sup>-1</sup> and 1592 cm<sup>-1</sup>, respectively.

The ID/IG ratio of 1.24 for the nanohybrid indicates a higher degree of defects, which is primarily due to the removal of functional groups from GO during the reduction process. There is no shift in La(OH)<sub>3</sub> modes, indicating electronic interactions between La(OH)<sub>3</sub> and graphene.

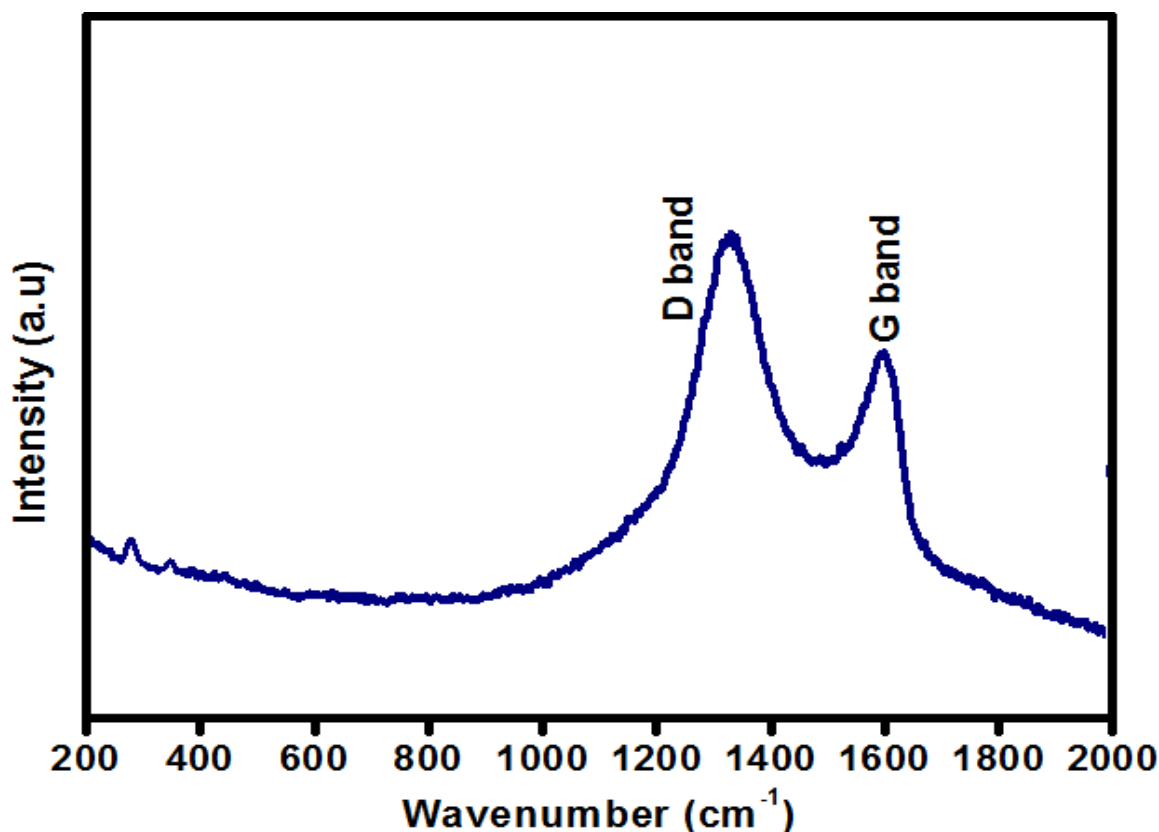
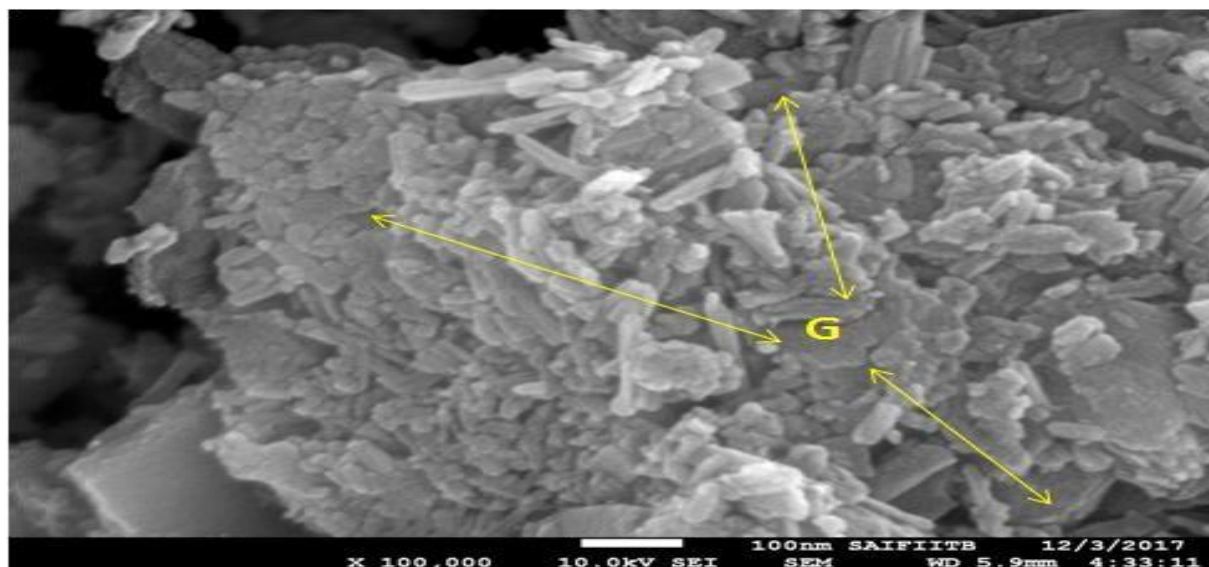


Fig.3.2. Raman spectrum of La(OH)<sub>3</sub>/G nanohybrid

### 3.3 FE-SEM studies

Fig. displays the FE-SEM image of the nanohybrid La(OH)<sub>3</sub>/G. The morphology of the La(OH)<sub>3</sub>/G hybrid is composed of graphene nanosheets distributed densely over La(OH)<sub>3</sub> nanoflakes. During the solvothermal reduction process, graphene oxide was reduced to graphene, which has more anchoring sites for in-situ growth of La(OH)<sub>3</sub> by electrostatic force, thereby preventing the formation of La(OH)<sub>3</sub> clusters and allowing for the restacking of graphene nanosheets.



**Fig. 3.3.** FE-SEM image of La(OH)<sub>3</sub>/G nanohybrid.

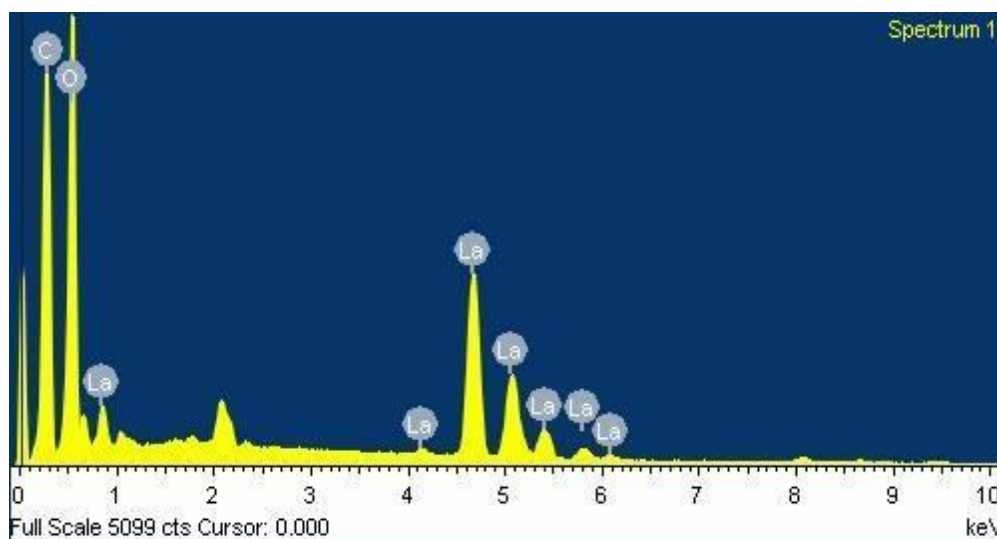


**Fig. 3.4.** Energy dispersive X-ray (EDX) spectra of La(OH)<sub>3</sub>/G nanohybrid.

Figure depicts the energy dispersive X-ray (EDX) spectrum of the nanohybrid La (OH)<sub>3</sub>/G. La (OH)<sub>3</sub>/G composite's EDX spectrum verifies the presence of carbon in the form of graphene in the La (OH)<sub>3</sub>/G nanohybrid. The mass ratio of La (OH)<sub>3</sub> to Graphene has been determined to be 1:0.5

#### 4. CONCLUSION



Electrochemical capacitors consist of two electrodes and an electrolyte separated by an ion-permeable membrane called a separator. Typically, as an electrode, materials with a thin coating on a current collector are utilised. To get optimum performance in a supercapacitor, it is necessary to choose an electrode with high electrical conductivity, good thermal stability, and a large surface area. An electrolyte dissolves substances that breakdown into ions, hence rendering it ionically conductive. This work demonstrates that the new porous microcubes morphological LNMO electrode materials are a potential contender as cathode materials for Li-ion battery and supercapacitor, which can be employed in the future for portable electronic devices with enhanced composition and electrolyte. Due to their unique characteristics such as high power density, high charge/discharge rates, and long cycle life, supercapacitors have been one of the most active fields of research. Compared to rechargeable batteries, the power density of supercapacitors was significantly higher. This makes supercapacitors an attractive electrochemical device for applications requiring a power surge. When compared to batteries in terms of charge/discharge rates, supercapacitors may be charged and drained in the least amount of time, which is a significant benefit. They also have a long cycle life, which can endure millions of cycles without undergoing an irreversible chemical reaction. Electric double-layer capacitance is a system that utilises the electric double-layer effect to store energy. This mechanism happens at the Helmholtz double layer contact between electrode and electrolyte. The amount of charge held in this interface is proportional to the applied voltage and is dependent on the nature, shape, and electrolyte type of the electrode surface. By regulating the surface area and pore size, it is possible to create a high capacitance for storage. Cost of materials, manufacturing, service life, environmental impact, and recyclability guide serious research and development of various energy conversion and storage devices. Therefore, for SCs to find a position in commercial applications, they must have a higher energy density and lower cost. Consequently, electrode materials play a significant role in enhancing the efficacy of an electrochemical capacitor. The following are the characteristics of an ideal electrode material for a supercapacitor's optimal efficacy: High specific surface area (which helps specific capacitance) Controlled porosity (which affects specific capacitance and rate capability) High electrical conductivity (which is essential to rate capability and power density) Desirable electroactive sites (which enables pseudo-capacitance) High thermal stability and chemical stability, which affect cycling stability.

## REFERENCES

1. F. Geng, Y. Matsushita, R. Ma, H. Xin, M. Tanaka, F. Izumi, et al., General synthesis and structural evolution of a layered family of  $\text{Ln}_8(\text{OH})_{20}\text{Cl}_4 \times n\text{H}_2\text{O}$  ( $\text{Ln} = \text{Nd}, \text{Sm}, \text{Eu}, \text{Gd}, \text{Tb}, \text{Dy}, \text{Ho}, \text{Er}, \text{Tm}, \text{and Y}$ ), *J. Am. Chem. Soc.* 130 (2008), 16344–16350.



2. H. Liu, P. He, Z. Li, Y. Liu, J. Li, A novel nickel-based mixed rare-earth oxide/activated carbon supercapacitor using room temperature ionic liquid electrolyte, *Electrochim. Acta.* 51 (2006), 1925–1931.
3. R. Della Noce, S. Eugénio, T.M. Silva, M.J. Carmezim, M.F. Montemor,  $\alpha$ -Co(OH)<sub>2</sub>/carbon nanofoam composite as electrochemical capacitor electrode operating at 2 v in aqueous medium, *J. Power Sources.* 288 (2015), 234–242.
4. J.P. Cheng, L. Liu, K.Y. Ma, X. Wang, Q.Q. Li, J.S. Wu, et al., Hybrid nanomaterial of  $\alpha$ -Co(OH)<sub>2</sub>nanosheets and few-layer graphene as an enhanced electrode material for supercapacitors, *J. Colloid Interface Sci.* 486 (2017), 344–350.
5. M. Suksomboon, J. Khuntilo, S. Kalasina, P. Suktha, J. Limtrakul, M. Sawangphruk, High-performance energy storage of Ag-doped Co(OH)<sub>2</sub>- coated graphene paper: In situ electrochemical X-ray absorption spectroscopy, *Electrochim. Acta.* 252 (2017), 91–100.
6. C. Zhao, F. Ren, X. Xue, W. Zheng, X. Wang, L. Chang, A high- performance asymmetric supercapacitor based on Co(OH)<sub>2</sub>/graphene and activated carbon electrodes, *J. Electroanal. Chem.* 782 (2016), 98–102.
7. L. Chang, F. Ren, C. Zhao, X. Xue, Synthesis of Co(OH)<sub>2</sub>/Ni(OH)<sub>2</sub>nanomaterials with excellent pseudocapacitive behavior and high cycling stability for supercapacitors, *J. Electroanal. Chem.* 778 (2016), 110–115.
8. F. Wang, S. Sun, Y. Xu, T. Wang, R. Yu, H. Li, High performance asymmetric supercapacitor based on Cobalt Nickle Iron-layered double hydroxide/carbon nanofibres and activated carbon, *Sci. Rep.* 7 (2017), 1–11.
9. G.W. Yang, C.L. Xu, H.L. Li, Electrodeposited nickel hydroxide on nickel foam with ultrahigh capacitance, *Chem. Commun.* 6 (2008), 6537- 6539.
10. Z. Lu, Z. Chang, W. Zhu, X. Sun, Beta-phased Ni(OH)<sub>2</sub> nanowall film with reversible capacitance higher than theoretical Faradic capacitance., *Chem. Commun. (Camb).* 47 (2011), 9651–9653.
11. X. Hu, S. Liu, C. Li, J. Huang, J. Luv, P. Xu, et al., Facile and environmentally friendly synthesis of ultrathin nickel hydroxide nanosheets with excellent supercapacitor performances, *Nanoscale.* 8 (2016), 11797- 11802.
12. H. Wang, X. Shi, W. Zhang, S. Yao, One-pot hydrothermal synthesis of flower-like  $\beta$ -Ni(OH)<sub>2</sub> encapsulated by reduced graphene oxide for high- performance supercapacitors, *J. Alloys Compd.* 711 (2017) 643-651.
13. R. Wang, A. Jayakumar, C. Xu, J.M. Lee, Ni(OH)<sub>2</sub> nanoflowers/graphene hydrogels: A new assembly for supercapacitors, *ACS Sustain. Chem. Eng.* 4 (2016), 3736–3742.